Dyes and Pigments 91 (2011) 99–104

Contents lists available at ScienceDirect

Dyes and Pigments

journal homepage: www.elsevier.com/locate/dyepig

Perylene diimide-appended mixed (phthalocyaninato)(porphyrinato) europium(III) double-decker complex: Synthesis, spectroscopy and electrochemical properties

Shuai Dong [a], Xianyao Zhang [a], Yang Zhou [a], Jianzhuang Jiang [a,b,*], Yongzhong Bian [b,**]

[a] Department of Chemistry, Shandong University, Jinan 250100, China
[b] Department of Chemistry, University of Science and Technology Beijing, Beijing 100083, China

A R T I C L E I N F O

Article history:
Received 6 January 2011
Received in revised form
6 March 2011
Accepted 7 March 2011
Available online 16 March 2011

Keywords:
Phthalocyanine
Porphyrin
Europium
Perylene diimide
Electrochemistry
Fluorescence spectrum

A B S T R A C T

Treatment of sandwich-type mixed (phthalocyaninato)(porphyrinato) metal complex [HEu^{III}\{Pc(α-3-OC_5H_{11})$_4$\}\{TriBPP(NH_2)\}] (**3**) [Pc(α-3-OC_5H_{11})$_4$ = 1,8,15,22-tetrakis(3-pentyloxy)-phthalocyaninate, TriBPP(NH_2) = 5,10,15-tris(4-*tert*-butylphenyl)-20-(4-aminophenyl)porphyrinate] with N-*n*-butyl-1,6,7,12-tetra(4-*tert*-butylphenoxyl)perylene-3,4-dicarboxylate anhydride-9,10-dicarboxylate imide (**2**) in the presence of imidazole in toluene afforded the novel perylene diimide-appended mixed (phthalocyaninato)(porphyrinato) europium(III) double-decker complex (**5**). Porphyrin–PDI dyad **4** was also obtained by similar method. The electronic absorption spectroscopic and electrochemical properties of PDI-appended double-decker **5** and the model compounds **2**, **3**, and **4** were studied, the results indicated that there was no considerable ground-state interaction between the double-decker unit and the PDI unit in **5**. The fluorescence measurements revealed that the emission of PDI unit was effectively quenched by the double-decker unit, suggesting remarkable intramolecular interaction in **5** under excited state.

1. Introduction

Light harvesting is a crucial part in natural photosynthetic process in which a series of highly efficient ultrafast energy transfers between spectroscopically different populations of chlorophylls are involved [1]. Several strategies have been employed to mimic the natural light-harvesting process, including the using of polymers [2], dendrimers [3], and porphyrin arrays linked by covalent bonds [4] or by self-assembly [5,6]. Photoinduced electron transfer is an important event not only in the primary process of natural photosynthesis [7] but also in some artificial systems such as molecular photovoltaics [8] and photocatalysis [9]. A variety of intramolecular and intermolecular photoinduced electron-transfer models have been investigated to elucidate the controlling factors [10–15].

Perylene diimide (PDI) derivatives [16] are well-known red pigments with outstanding stability, intense absorption in the 400–600 nm region, and high fluorescence emission. Due to the high electron affinity caused by the electron-withdrawing imide groups, PDIs are also good electron acceptors in artificial photosynthetic models [10,17,18]. Moreover, they are good n-type organic semiconductor materials and widely used as building blocks in various molecular electronic devices [19,20] and self-assembled nanocomposite [21–24].

On the other hand, porphyrin derivatives, including their most important artificial analogues, phthalocyanines, are known to have unique π-conjugated structural features which are closely related to that of bacteriochlorophyll in the reaction center, thus they can be used as excellent light-harvesting antennas [25,26]. They also produce efficient photoinduced electron-transfer processes that can be regulated by the appropriate choice of the central metal and the nature of the peripheral substitution. In this regard, considerable efforts have been devoted to multiporphyrin arrays and hetero-porphyrin–phthalocyanine arrays linked by covalent bond or supramolecular interactions [11–14,27–33]. Sandwich-type porphyrinato and phthalocyaninato metal complexes have also been extensively studied [34–36]. Due to their face-to-face proximity of the tetrapyrrole ligands, these sandwich-type tetrapyrrole metal complexes show notable decrease of the first oxidation

---

[*] Corresponding author. Department of Chemistry, University of Science and Technology Beijing, Beijing 100083, China. Tel.: +86 (0)10 6233 2592; fax: +86 (0) 10 6233 2462.

[**] Corresponding author.
E-mail addresses: jzjiang@sdu.edu.cn (J. Jiang), yzbian@ustb.edu.cn (Y. Bian).

0143-7208/$ – see front matter © 2011 Elsevier Ltd. All rights reserved.
doi:10.1016/j.dyepig.2011.03.010

potentials and increase of the first reduction potentials as compared with the respective mono(tetrapyrrole) compounds. As a result, they can serve as potent electron donors [37], electron acceptors [38] and both roles [39], respectively, in charge-transfer materials. Covalently linked electron donor–acceptor systems involving sandwich-type bis(porphyrinate) metal unit were first reported in 1996 with a quinine [40,41] or a pyromellitic imide [40] chromophore as the electron-acceptor partner. In 2007, the photophysical properties for a series of porphyrin-appended bis(phthalocyaninato) europium complexes having different number of porphyrin-substituents at the peripheral or non-peripheral position(s) of the phthalocyanine ligand were examined for the first time by this group [42]. A rapid and efficient photoinduced electron-transfer process from the porphyrin unit(s) to $[Eu(Pc)_2]$ core was revealed. Torres and co-workers synthesized a series of heterodyads composed of bis(phthalocyaninato) rare earth double-decker unit covalently linked to C_{60} and studied their photophysics [43]. They found that photoexcitation of C_{60} leads to a rapid electrotransfer from the double-decker unit to the C_{60} and a charge-separated state, $[RE^{III}(Pc)(Pc')]^{+}$-$C_{60}{}^{-}$, with lifetime longer than 3 ns. Very recently, a series of mixed (phthalocyaninato)(porphyrinato) yttrium double-decker complexes having one metal-free porphyrin chromophore linked at the *para*, *meta*, and *ortho* position, respectively, of one meso-phenyl group of the porphyrin ligand in the double-decker unit, were synthesized by us [44]. Comparative studies over these three isomeric tetrapyrrole triads by steady-state and transient spectroscopic methods clearly reveal the effect of the position of porphyrin-substituent on the photophysical properties of the triads.

In the present paper, we report the synthesis, spectroscopic and electrochemical properties of a novel mixed (phthalocyaninato)(-porphyrinato) europium(III) double-decker complexes appended with one PDI chromophore at the *para* position of one meso-phenyl group of the porphyrin ligand in the double-decker unit through imide linkage, **5**, Scheme 1. The corresponding data for model compounds, 5,10,15-tris(4-*tert*-butylphenyl)-20-(4-aminophenyl)porphyrin $[H_2TriBPP(NH_2)]$ (**1**), N-*n*-butyl-1,6,7,12-tetra(4-*tert*-butylphenoxyl) perylene-3,4-dicarboxylate anhydride-9,10-dicarboxylate imide (**2**), $[HEu^{III}\{Pc(\alpha\text{-}3\text{-}OC_5H_{11})_4\}\{TriBPP(NH_2)\}]$ (**3**) $[Pc(\alpha\text{-}3\text{-}OC_5H_{11})_4 =$ 1,8,15,22-tetrakis(3-pentyloxy)-phthalocyaninate, $TriBPP(NH_2) =$ 5,10,15-tris(4-*tert*-butylphenyl)-20-(4-aminophenyl)porphyrinate], and porphyrin–PDI dyad **4**, have also been measured and discussed for comparison.

2. Experimental section

2.1. General

n-Octanol was distilled from sodium under nitrogen. Column chromatography was carried out on silica gel (Merck, Kieselgel 60, 70–230 mesh) and biobeads (BIORAD S-X1, 200–400 mesh) columns with the indicated eluents. All other reagents and solvents were used as received. The compounds $Eu(acac)_3 \cdot nH_2O$ [45], 1,8,15,22-tetrakis (3-pentyloxy)-phthalocyanine [46], 5,10,15-tris(4-*tert*-butylphenyl)-20-(4-aminophenyl)porphyrin (**1**) [47] and N-*n*-butyl-1,6,7,12-tetra(4-*tert*-butylphenoxyl) perylene-3,4-dicarboxylate anhydride-9,10-dicarboxylate imide (**2**) [48] were prepared according to the published procedures.

2.2. Measurement

^{1}H NMR spectra were recorded on a Bruker DPX 300 spectrometer (300 MHz) in $CDCl_3$, [D6] DMSO, or $CDCl_3$/[D6] DMSO 1:1. Spectra were referenced internally by using the residual solvent resonance ($\delta = 7.26$ and 2.49 ppm for $CDCl_3$ and [D6] DMSO, respectively) relative to $SiMe_4$ (TMS). MALDI-TOF mass spectra

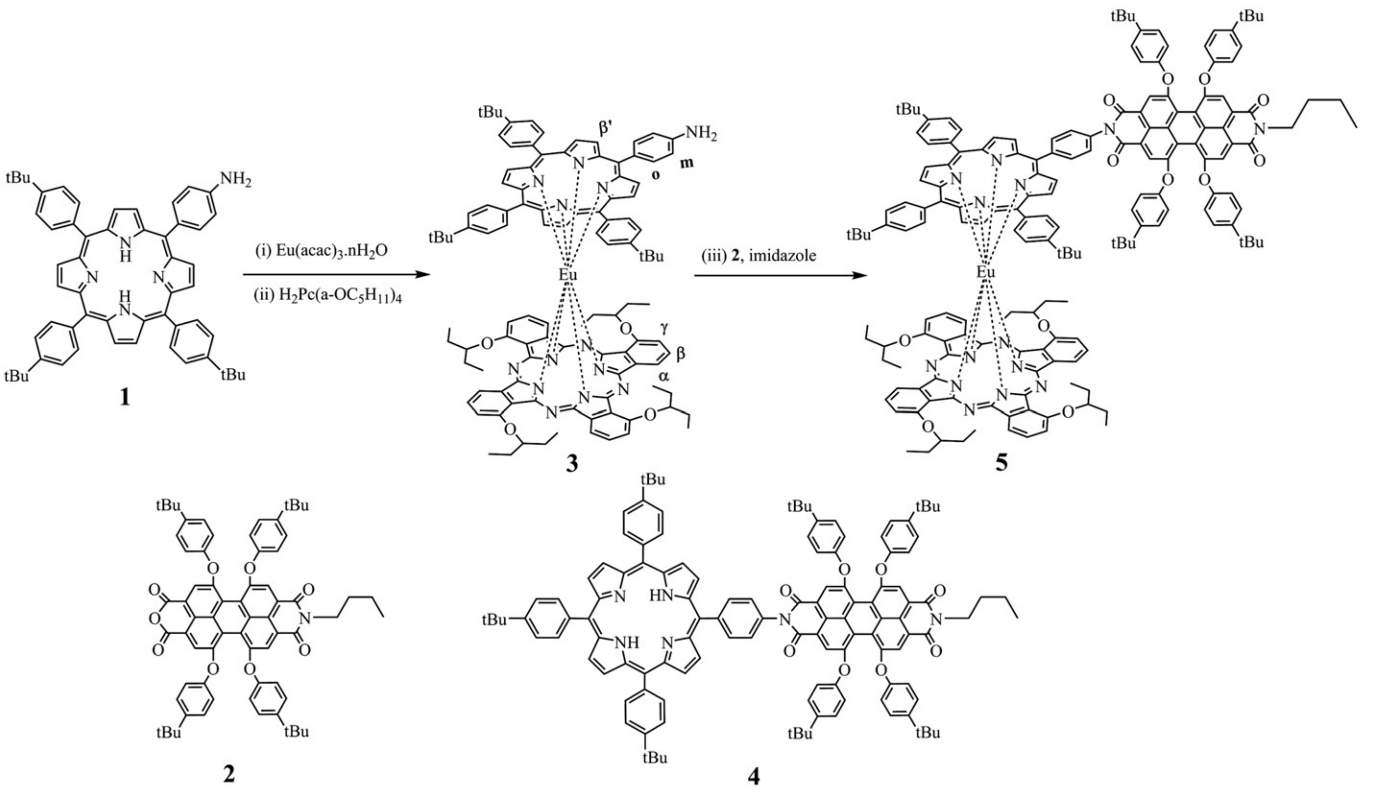

Scheme 1. Synthesis of the PDI-appended double-decker **5** and the schematic molecular structures of compounds **2** and **4**.

were taken on a Bruker BIFLEX III ultra-high resolution Fourier transform ion cyclotron resonance (FTICR) mass spectrometer with alpha-cyano-4-hydroxycinnamic acid as the matrix. Elemental analyses were performed on an Elementar Vavio El III. Electronic absorption spectra were obtained with a Hitachi U-4100 spectrophotometer. The steady-state emission spectra were measured by an Edinburgh FS920 Fluorescence Spectrophotometer. Solutions were prepared in $CHCl_3$ with concentration of 21.1 μM for **2**, 5.6 μM for **3**, and 7.3 μM for **5**. Electrochemical measurements were carried out with a BAS CV-50W voltammetric analyzer. The cell comprised inlets for a glassy carbon disk working electrode of 2.0 mm in diameter and a silverwire counter electrode. The reference electrode was Ag/Ag^+ (a solution of 0.01 M $AgNO_3$ and 0.1 M TBAP in acetonitrile), which was connected to the solution by a Luggin capillary whose tip was placed close to the working electrode. It was corrected for junction potentials by being referenced internally to the saturated calomel electrode (SCE). Typically, a 0.1 M solution of $[NBu_4][ClO_4]$ in CH_2Cl_2 containing 0.5 mM of sample was purged with nitrogen for 10 min, and then the voltammograms were recorded at ambient temperature. The scan rate was 20 and 10 mV s^{-1} for CV and DPV, respectively.

2.3. Preparation of $HEu^{III}[Pc(\alpha\text{-}3\text{-}OC_5H_{11})_4][TriBPP(NH_2)]$ (**3**)

A mixture of $[Eu(acac)_3]\cdot nH_2O$ (51.4 mg, 0.11 mmol) and $H_2TriBPP$ (79.8 mg, 0.10 mmol) in *n*-octanol was heated to reflux under nitrogen for 4 h. After the mixture was cooled to room temperature, $H_2Pc(\alpha\text{-}3\text{-}OC_5H_{11})_4$ (86.0 mg 0.10 mmol) was added and then heated to reflux for another 2 h. After a brief cooling, the solvent was evaporated under reduced pressure, and the residue was dissolved in $CHCl_3/CH_3OH$ (1:1, v/v). Then, hydrazine hydrate (300 mg) was added, and the mixture was rotary evaporated to dryness. The residue was subjected to chromatography on a silica-gel column. A small amount of metal-free $H_2TriBPP(NH_2)$ was separated by using $CHCl_3$/hexane (1:2) as the eluent, and then the column was eluted with $CHCl_3$. A small green band containing metal-free phthalocyanine followed by another green band containing the protonated double-decker was developed. Repeated chromatography followed by recrystallization from $CHCl_3/CH_3OH$ gave pure **3** as deep green powder (43 mg, 20%). ^1H NMR (300 MHz, $CDCl_3$/[D6] DMSO (1:1) with ca. 1% hydrazine hydrate, 25 °C, TMS): $\delta = 10.8$ (s, 4H; Pc H_α), 9.90 (s, 4H; Pc H_β), 8.71 (s, 4H; Pc H_γ), 8.43 (s, 6H; Por $H_{\beta 1}$), 7.95 (s, 6H; Por H_{o1}), 7.45 (s, 2H; Por $H_{\beta 2}$), 7.30 (s, 6H; Por H_{m1}), 7.15 (s, 2H; Por H_{o2}), 6.13 (d, 4H; OCH), 5.89 (s, 2H; Por NH_2), 3.29 (t, $J = 6.6$ Hz, 8H; Por NCH_2), 2.56 (m, $J = 7.2$ Hz, 8H; Por $NCH_2CH_2C_6H_{13}$), 2.18 (m, $J = 6.6$ Hz, 8H; Pc endo-CH_2), 1.82 (m, $J = 6.6$ Hz, 8H; Pc exo-CH_2), 1.69 (t, $J = 7.5$ Hz, 12H; Pc endo-CH_3), 1.59–1.40 (brd, 40H; Por CH_3), 1.24 (t, $J = 7.5$ Hz, 12H; Pc exo-CH_3), 0.97 (t, $J = 6.6$ Hz, 12H; Por CH_3); MS (MALDI-TOF): an isotopic cluster peaking at *m*/*z*: 1807.0; calcd. for $(MH)^+$: 1806.8. Anal. calcd. for $C_{108}H_{111}N_{13}O_4Eu$: C, 70.09; H, 6.46; N, 9.57. Found: C, 69.55; H, 6.49; N, 9.65.

2.4. Preparation of porphyrin–PDI dyad (**4**)

A mixture of $H_2TriBPP(NH_2)$ (**1**) (40 mg, 0.05 mmol) and PDI **2** (50 mg, 0.05 mmol) in dry toluene in the presence of imidazole (500 mg) was heated to reflux under nitrogen for 12 h. The resulting solution was cooled and the solvent was removed under reduced pressure. The residue was dispersed in water and filtered to remove imidazole. The residue was washed with water and purified by chromatography on a silica-gel column with $CHCl_3$ as the eluent to give a crude product. The crude product was further purified by repeated chromatography and recrystallization from $CHCl_3/CH_3OH$ to give **4** as red powder (5.0 mg, 5.6%). ^1H NMR (300 MHz, $CDCl_3$, 25 °C, TMS): $\delta = 8.91$–8.88 (m, 8H; $H_{pyrrole}$), 8.39 (s, 2H; H_{per}), 8.35 (d, $J = 8.1$ Hz, 2H; H_{por}), 8.29 (s, 2H; H_{per}), 8.16–8.12 (d, $J = 8.4$ Hz, 6H; H_{por}), 7.76 (d, $J = 8.1$ Hz, 6H, H_{por}), 7.65 (d, $J = 8.1$ Hz, 2H; H_{por}), 7.29 (m, 8H; H_{ar}), 6.92 (m, 4H; H_{ar}), 6.89 (m, 4H; H_{ar}), 4.14 (m, 2H; CH_2), 1.61 (m, 27H; CH_3), 1.43 (m, 4H; CH_2), 1.31 (s, 36H; CH_3), 0.96 (m, 3H; CH_3), −2.78 (s, 2H, H_{por}); MS (MALDI-TOF): an isotopic cluster peaking at *m*/*z*: 1821.0; calcd. for $(MH)^+$: 1821.3.

2.5. Preparation of perylene diimide-appended mixed (phthalocyaninato)(porphyrinato) europium(III) double-decker complex (**5**)

A mixture of $HEu^{III}[Pc(\alpha\text{-}3\text{-}OC_5H_{11})_4][TriBPP(NH_2)]$ **(3)** (50 mg, 0.028 mmol) and PDI **2** (40 mg, 0.04 mmol) in dry toluene in the presence of imidazole (500 mg) was heated to reflux under nitrogen for 12 h. The resulting solution was cooled and the solvent was removed under reduced pressure. The residue was dispersed in water and filtered to remove imidazole. The residue was washed with water and purified by chromatography on a silica-gel column with $CHCl_3$ as the eluent to give a crude product. The crude product was further purified by repeated chromatography and recrystallization from $CHCl_3/CH_3OH$ to give **5** as deep red powder (3.0 mg, 3.3%). MS (MALDI-TOF): an isotopic cluster peaking at *m*/*z*: 2828.4; calcd. for $(MH)^+$: 2828.3.

3. Results and discussion

3.1. Synthesis and characterization

As shown in Scheme 1, the synthesis of mixed (phthalocyaninato)(porphyrinato) rare earth double-decker complexes $[HEu^{III}\{Pc(\alpha\text{-}3\text{-}OC_5H_{11})_4\}\{TriBPP(NH_2)\}]$ (**3**) involves the prior generation of the half-sandwich complexes $[Eu^{III}(acac)\{TriBPP(NH_2)\}]$ from $[Eu^{III}(acac)_3\cdot nH_2O]$ and $[H_2TriBPP(NH_2)]$ (**1**), followed by treatment with metal-free phthalocyanine $[H_2Pc(\alpha\text{-}3\text{-}OC_5H_{11})_4]$. It is worth noting that the reaction produces a mixture of the neutral form $[Eu^{III}\{Pc(\alpha\text{-}3\text{-}OC_5H_{11})_4\}\{TriBPP(NH_2)\}]$ and the protonated form $[HEu^{III}\{Pc(\alpha\text{-}3\text{-}OC_5H_{11})_4\}\{TriBPP(NH_2)\}]$ of the target compounds [49–51]. The neutral form of this type of double-decker is less stable than the protonated species. For easy processing, the reaction mixture was treated with hydrazine hydrate prior to isolation and purification to convert the neutral form into the corresponding protonated one. Treatment of **3** with N-*n*-butyl-1,6,7,12-tetra(4-*tert*-butylphenoxyl)perylene-3,4-dicarboxylate anhydride-9,10-dicarboxylate imide (**2**) in the presence of imidazole in toluene afforded the PDI-appended double-decker **5**. By using the above procedure with metal-free porphyrin $[H_2TriBPP(NH_2)]$ (**1**) instead of double-decker complex (**3**) as the starting material, the PDI-Por dyad **4** was obtained [6].

The newly synthesized compounds are soluble in common organic solvents such as CH_2Cl_2, $CHCl_3$, and toluene, allowing characterization of these compounds by MALDI-TOF mass and ^1H NMR spectroscopy. MALDI-TOF MS spectra of compounds **3**–**5** show intense signals of protonated molecular ions $[MH^+]$, Figs. S1 and S2 in the Supporting information. The isotopic pattern closely resembled the simulated one as exemplified by the spectrum of **5** given in Fig. 1, providing evidence for the identity of the PDI-appended double-decker compound. Well-resolved ^1H NMR spectra of compound **4** in $CDCl_3$ were recorded and assigned, see Experimental section for detail. Satisfactory NMR spectra could not be obtained for either the protonated double-decker **3** or the dyad **5** containing the protonated double-decker unit in $CDCl_3$, [D6] DMSO, or a mixed solvent of $CDCl_3$/[D6] DMSO (1:1), due to the tautomerization of the acidic proton on the porphyrin ligand in the

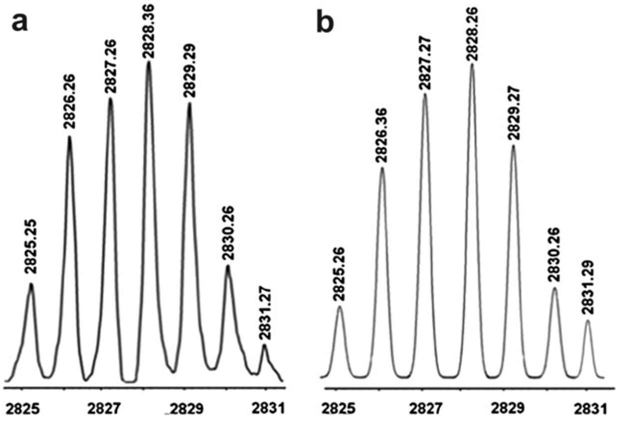

Fig. 1. (a) Experimental and (b) simulated isotopic pattern for $[MH]^+$ of **5** shown in the MALDI-TOF mass spectrum.

double-decker unit [44]. Upon addition of ca. 1% hydrazine hydrate, the double-decker unit was reduced to the corresponding monoanion [52], thereby making the two macrocyclic ligands become diamagnetic, and well-resolved spectra with virtually all the expected signals were observed for **3**, Fig. S3 (Supporting information). However, most probably due to the relatively poor solubility in $CDCl_3$/[D6] DMSO (1:1), ^1H NMR spectra of compound **5** remain unresolved.

3.2. Steady-state electronic absorption spectra

The electronic absorption data of compounds **2**–**5** were measured in $CHCl_3$ and compiled in Table 1. Fig. 2 compares the electronic absorption spectra of **2**, **3** and **5**. PDI derivative **2** shows a typical electronic absorption feature with two intense bands at 584 and 454 nm, along with a shoulder peak at 543 nm, which is typical for PDIs with four bay positions substituted [48]. The electronic absorption spectrum of mixed bis(porphyrinato)(phthalocyaninato) europium compound **3** resembled those of HMPc[(α-3-OC_5H_{11})$_4$](TClPP) [M = Y, Sm, Eu; TClPP = meso-tetrakis(4-chlorophenyl)porphyrinate] [49], HY^{III}Pc[(α-3-OC_5H_{11})$_4$](TOAPP) [TOAPP = meso-tetrakis(4-octylamino-phenyl)porphyrinate] [51] and HM[Pc(OBNP)$_2$](TClPP) (M = Y, Eu; Pc(OBNP)$_2$ = binaphthylphthalocyaninate) [50], indicating the protonated mixed ring double-decker nature of this complex. The spectrum shows medium-to-strong phthalocyanine and porphyrin soret bands at 311 and 414 nm, respectively, and several Q bands in the range of 500–900 nm in addition to a band with medium intensity at 488 nm attributed to a transition involving a delocalized orbital.

In the electronic absorption spectrum of the PDI-appended double-decker **5**, the absorption bands at 414, 489, 642, 865 nm are attributed to the double-decker unit, while the band at 455 nm is assigned to the PDI unit. The other two bands peaked at 543, 587 nm, respectively, are believed to have contribution from both the double-decker and PDI units. It is noteworthy that the spectrum of **5** is very similar to a linear superimposition of those of the individual components **2** and **3**, Fig. 2. This observation suggests the absence of a strong electronic interaction between the double-decker and PDI components in **5** at ground state. This seems also true for the PDI-Por dyad **4**, which can be revealed by comparing the electronic absorption spectra of compounds **1**, **2** and **4**, Fig. S4 (Supporting information). The results are consistent with previous reports on similar system [6,42–44].

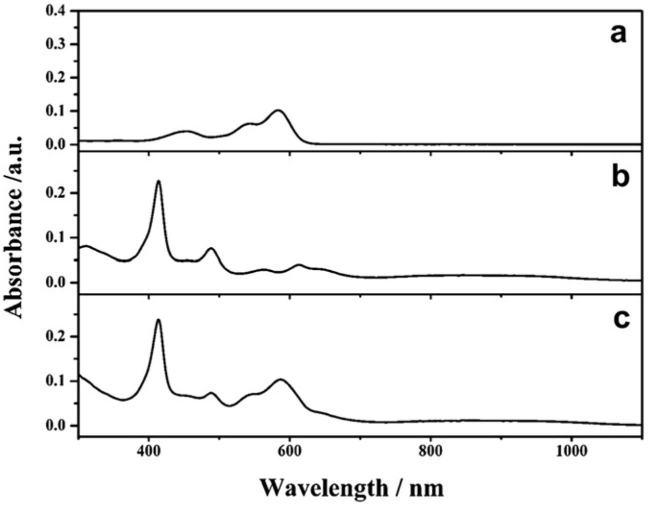

Fig. 2. Electronic absorption spectra of the compounds **2** (a), **3** (b), and **5** (c) in 1.0×10^{-6} M $CHCl_3$ solution.

3.3. Electrochemical properties

The electrochemical behavior of compounds **2**–**5** was investigated by cyclic voltammetry (CV) and differential pulse voltammetry (DPV) in CH_2Cl_2, Fig. S5. The half-wave redox potential values vs. the saturated calomel electrode (SCE) were summarized in Table 2. The separation between the reduction and oxidation peak potentials for all the processes lies between 65 and 90 mV, showing their reversible nature. All these processes can be attributed to successive removal from or addition of electron(s) to the molecular orbitals.

The PDI derivative **2** displays two one-electron oxidations, labeled as Oxd1 (1.29 V) and Oxd2 (1.58 V), and two one-electron reductions labeled as Red1 (−0.69 V) and Red2 (−0.86 V) within the electrochemical window of CH_2Cl_2. The double-decker complex **3** shows two one-electron reductions at −0.89 and −1.70 V, and up to four one-electron oxidations at 0.43, 0.98, 1.67, and 1.99 V. A direct comparison of the electrochemical data of **5** with those of **2** and **3** helps to assign the origin of the redox processes to the double-decker and PDI components for **5**. Accordingly, the oxidations at 0.34, 0.88 and 1.98 V can be attributed to the double-decker component, the reduction at −0.59 V to the PDI component, while the redox couples at 1.51, −0.98, and −1.34 V have contributions from both the double-decker and PDI components.

Table 1
Electronic absorption data for compounds **1**–**5** in $CHCl_3$.

Compound	λ_{max} [nm] (log ϵ)							
1		420 (5.83)		516 (4.50)	552 (4.34)	591 (4.18)	648 (4.22)	
2			454 (4.17)		543 (4.37)	584 (4.59)		
3	311 (4.84)	414 (5.30)		488 (4.81)	563 (4.35)	613 (4.51)	642 (4.38)	865 (4.05)
4		420 (5.72)	455 (4.31)	520 (4.53)	552 (4.64)	590 (4.81)	648 (3.83)	
5	293 (4.82)	414 (5.12)	455 (4.57)	489 (4.61)	543 (4.58)	587 (4.76)	642 (4.21)	865 (3.80)

Table 2
Half-wave redox potentials of **2**–**5** (V vs. SCE) in CH_2Cl_2 containing 0.1 M tetrabutylammonium perchlorate recorded by DPV.

Compound	Red4	Red3	Red2	Red1	Oxd1	Oxd2	Oxd3	Oxd4	$\Delta E^o_{1/2}$[a]
H_2TBPP[b]			−1.56	−1.21	0.94	1.18	1.34	1.60	2.15
2			−0.86	−0.69	1.29	1.58			1.98
3			−1.70	−0.89	0.43	0.98	1.67	1.99	1.32
4	−1.56	−1.20	−0.88	−0.72	0.96	1.31	1.58		1.68
5		−1.34	−0.98	−0.59	0.34	0.88	1.51	1.98	0.93

[a] $\Delta E^o_{1/2} = E_{1/2}(Oxd1) - E_{1/2}(Red1)$.
[b] Cited from Ref. [53].

For comparison, the electrochemical data of 5,10,15,20-tetra(4-*tert*-butylphenyl)-porphyrin (H_2TBPP) [53] are also listed in Table 2, which shows two one-electron reductions at −1.21 and −1.56 V, and four one-electron oxidations at 0.94, 1.18, 1.34 and 1.60 V. Taking the data of PDI derivative **2** into account, similar assignment for the electrochemical data of PDI-Por dyad **4** can be made. Thus, the reductions at −1.20 and −1.56 V, and the oxidation at 0.96 V are assigned to the porphyrin moiety, the two reductions at −0.72 and −0.88 V are attributed to the PDI moiety, the remaining two oxidations at 1.31 and 1.58 V are related to both the porphyrin and PDI moieties.

3.4. *Fluorescence spectra*

In order to study the intramolecular electronic interactions for the PDI-appended double-decker **5**, the fluorescence measurements were carried on compounds **2**, **3** and **5** in $CHCl_3$. It is well know that metal-free porphyrins usually show two strong emission bands around 650 and 720 nm [44], respectively. On the other hand, sandwich-type tetrapyrrole rare earth complexes always show very weak or actually no fluorescence, due to the heavy rare earth atom effect and strong electronic interaction between the neighboring tetrapyrrole rings in the sandwich molecules [37–44]. Similarly in the present work, it was found that the fluorescence of double-decker complex **3** was completely quenched.

The fluorescence spectra of compounds **2** and **5** are shown in Fig. 3. With excitation at 456 nm, the PDI derivative **2** shows one strong emission band centered at 619 nm, which is consistent with the previous reports on similar compounds [6,48]. Whereas for the PDI-appended double-decker **5**, this emission band is remarkably quenched, and no other emission band can be observed. Since the double-decker moiety is easily oxidized and may act as excellent electron donor [43], and the PDI moiety is readily reduced and may serve as good electron acceptor [6], a concomitant photoinduced electron transfer seems to account for the fluorescence quenching process. On the other hand, because of the good spectral overlap between the emission of PDI derivative **2** and the absorptions of the double-decker complex **3**, there is a possibility of a photoinduced intramolecular singlet–singlet energy-transfer process from the excited PDI chromophore to the double-decker unit. For further identify the responsible process for the fluorescence quenching, the time-resolved absorption and fluorescence spectra are under investigation.

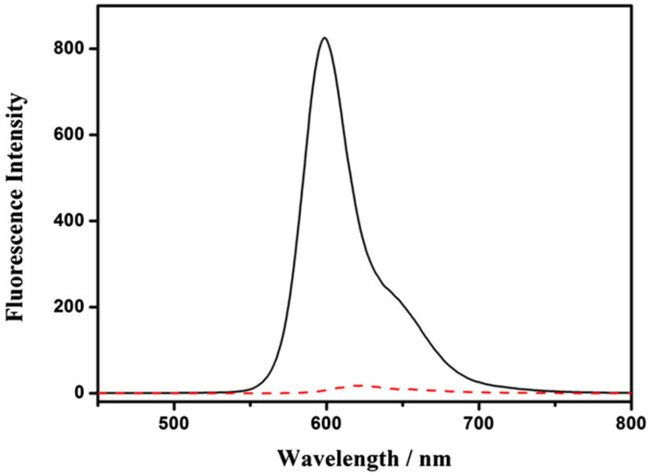

Fig. 3. Fluorescence spectra of compounds **2** (solid line) and **5** (dashed line) in $CHCl_3$ (normalized with matching absorption of 0.1 at the 456 nm excitation wavelength).

4. Conclusion

A novel phthalocyanine–porphyrin–PDI array containing a sandwich-type mixed (phthalocyaninato)(porphyrinato) europium(III) double-decker core and a PDI modifier was designed and synthesized. The steady-state electronic absorption and electrochemical studies indicated that there was no ground-state interaction between the double-decker unit and the PDI unit. The fluorescence measurements revealed that the emission of PDI unit was remarkably quenched by the double-decker unit. The preliminary result suggests that the PDI-appended double-decker **5** would show very novel photophysical properties, which are worth of further investigation.

Acknowledgments

Financial support from the Natural Science Foundation of China, the Fundamental Research Funds for the Central Universities, Beijing Natural Science Foundation is gratefully acknowledged.

Appendix A. Supplementary data

MALDI-TOF mass spectra of compounds **4** and **5**; ^1H NMR spectra of $HEu^{III}[Pc(\alpha\text{-}3\text{-}OC_5H_{11})_4][TriBPP(NH_2)]$ (**3**) in $CDCl_3$/[D6] DMSO (1:1) upon addition of ca. 1% hydrazine hydrate; electronic absorption spectra of the compounds **1**, **2** and **4** in $CHCl_3$; differential pulse voltammograms (DPV) of compounds **2** and **4** in CH_2Cl_2 containing 0.1 M $[Bu_4N][ClO_4]$. This material can be found in the, online version at, doi:10.1016/j.dyepig.2011.03.010 or from the authors.

References

[1] Sundström V, Pullerits T, van Grondelle R. Photosynthetic light-harvesting: reconciling dynamics and structure of purple bacterial LH2 reveals function of photosynthetic unit. J Phys Chem B 1999;103:2327–46.
[2] Webber SE. Photon-harvesting polymers. Chem Rev 1990;90:1469–82.
[3] Frechet JM. Dendrimers and other dendritic macromolecules: from building blocks to functional assemblies in nanoscience and nanotechnology. J Polym Sci Part A Polym Chem 2003;41:3713–25.
[4] Imahori H. Giant multiporphyrin arrays as artificial light-harvesting antennas. J Phys Chem B 2004;108:6130–43.
[5] Takahashi R, Kobuke Y. Hexameric macroring of gable-porphyrins as a light-harvesting antenna mimic. J Am Chem Soc 2003;125:2372–3.

[6] van der Boom T, Hayes RT, Zhao Y, Bushard PJ, Weiss EA, Wasielewski MR. Charge transport in photofunctional nanoparticles self-assembled from zinc 5,10,15,20-tetrakis(perylenediimide)porphyrin building blocks. J Am Chem Soc 2002;124:9582–90.
[7] Deisenhofer J, Norris JR, editors. The photosynthetic reaction center. San Diego, CA: Academic; 1993.
[8] Brabec C, Dyakonov V, Parisi J, Sariciftci NS, editors. Organic photovoltaics. Berlin, Germany: Springer; 2003.
[9] Balzani V, editor. Electron transfer in chemistry. Weinheim, Germany: Wiley-VCH; 2001.
[10] Wasielewski MR. Photoinduced electron transfer in supramolecular systems for artificial photosynthesis. Chem Rev 1992;92:435–61.
[11] Wasielewski MR. Self-assembly strategies for integrating light harvesting and charge separation in artificial photosynthetic systems. Acc Chem Res 2009;42:1910–21.
[12] Aratani N, Kim D, Osuka A. Discrete cyclic porphyrin arrays as artificial light-harvesting antenna. Acc Chem Res 2009;42:1922–34.
[13] Gust D, Moore TA, Moore AL. Mimicking photosynthetic solar energy transduction. Acc Chem Res 2001;34:40–8.
[14] Holten D, Bocian DF, Linsey JS. Probing electronic communication in covalently linked multiporphyrin arrays. A guide to the rational design of molecular photonic devices. Acc Chem Res 2002;35:57–69.
[15] Blanco MJ, Jiménez MC, Chambron JC, Heitz V, Linke M, Sauvage JP. Rotaxanes as new architectures for photoinduced electron transfer and molecular motions. Chem Soc Rev 1999;28:293–305.
[16] Zollinger H. Color chemistry. 3rd ed. Weinheim: VCH; 2003.
[17] Xu W, Chen H, Wang Y, Zhao C, Li X, Wang S, et al. Photoinduced electron and energy transfer in dyads of porphyrin dimer and perylene tetracarboxylic diimide. ChemPhysChem 2008;9:1409–15.
[18] Wu H, Wang H, Xue L, Shi Y, Li X. Hindered intramolecular electron transfer in room-temperature ionic liquid. J Phys Chem B 2010;114:14420–5.
[19] Dimitrakopoulos CD, Malenfant PRL. Organic thin film transistors for large area electronics. Adv Mater 2002;14:99–117.
[20] Wang Y, Chen Y, Li R, Wang S, Su W, Ma P, et al. Amphiphilic perylenetretracarboxyl diimide dimer and its application in field effect transistor. Langmuir 2007;23:5836–42.
[21] Würthner F. Perylene bisimide dyes as versatile building blocks for functional supramolecular architectures. Chem Commun; 2004:1564–79.
[22] Li X, Sinks LE, Rybtchinski B, Wasielewski MR. Ultrafast aggregate-to-aggregate energy transfer within self-assembled light-harvesting columns of zinc phthalocyanine tetrakis(perylenediimide). J Am Chem Soc 2004;126:10810–1.
[23] Chen Y, Chen L, Qi G, Wu H, Zhang Y, Xue L, et al. Self-assembled organic–inorganic hybrid nanocomposite of a perylenetetracarboxylic diimide derivative and CdS. Langmuir 2010;26:12473–8.
[24] Indelli MT, Chiorboli C, Scandola F, Iengo E, Osswald P, Würthner F. Photoinduced processes in self-assembled porphyrin/perylene bisimide metallosupramolecular boxes. J Phys Chem B 2010;114:14495–504.
[25] Chou JH, Nalwa HS, Kosal ME, Rakow NA, Suslick KS. Applications of porphyrins and metalloporphyrins to materials chemistry. In: Kadish KM, Smith KM, Guilard R, editors. The porphyrin handbook, vol. 6. San Diego: Academic Press; 2000. p. 43–132.
[26] Li X, Wang H, Wu H. Phthalocyanines and their analogues applied in dye sensitized solar cell. Struct Bond 2010;135:229–74.
[27] De la Escosura A, Martinez-Diaz MV, Guldi DM, Torres T. Stabilization of charge-separated states in phthalocyanine–fullerene ensembles through supramolecular donor–acceptor interactions. J Am Chem Soc 2006;128:4112–8.
[28] D'Souza F, Subbaiyan NK, Xie Y, Hill JP, Ariga K, Ohkubo K, et al. Anion-complexation-induced stabilization of charge separation. J Am Chem Soc 2009;131:16138–46.
[29] Lo PC, Leng X, Ng DKP. Hetero-arrays of porphyrins and phthalocyanines. Coord Chem Rev 2007;251:2334–53.
[30] Winters MU, Dahlstedt E, Blades HE, Wilson CJ, Frampton MJ, Anderson HL, et al. Probing the efficiency of electron transfer through porphyrin-based molecular wires. J Am Chem Soc 2007;129:4291–7.
[31] Cho HS, Rhee H, Song JK, Min CK, Takase M, Aratani N, et al. Excitation energy transport processes of porphyrin monomer, dimer, cyclic trimer, and hexamer probed by ultrafast fluorescence anisotropy decay. J Am Chem Soc 2003;125:5849–60.
[32] Peng X, Aratani N, Takagi A, Matsumoto T, Kawai T, Hwang IW, et al. A dodecameric porphyrin wheel. J Am Chem Soc 2004;126:4468–9.
[33] Li X, Ng DKP. Self-assembly of meso-pyridylporphyrins and zinc phthalocyanines through axial coordination. Eur J Inorg Chem; 2000:1845–8.
[34] Buchler JW, Ng DKP. Metal tetrapyrrole double- and triple-deckers with special emphasis on porphyrin systems. In: Kadish KM, Smith KM, Guilard R, editors. The porphyrin handbook, vol. 3. San Diego: Academic Press; 2000. p. 245–94.
[35] Weiss R, Fischer J. Lanthanide phthalocyanine complexes. In: Kadish KM, Smith KM, Guilard R, editors. The porphyrin handbook, vol. 16. San Diego: Academic Press; 2003. p. 171–246.
[36] Jiang J, Ng DKP. A decade journey in the chemistry of sandwich-type tetrapyrrolato-rare earth complexes. Acc Chem Res 2009;42:79–88.
[37] Capobianchi A, Ercolani C, Paoletti AM, Pennesi G, Rossi G, Chiesi-Villa A, et al. Interligand carbon–carbon.sigma.-bond breaking and repair in a "stapled" bis(phthalocyaninato)titanium complex. Synthesis, characterization, and electrical conductivity properties of oxidation products of bis(phthalocyaninato)titanium(IV) and bis(phthalocyaninato)tin(IV) and X-ray crystal structure of [Pc2Ti](I3)0.66. Inorg Chem 1993;32:4605–11.
[38] Galmiche L, Mentec A, Pondaven A, L'Her M. Charge transfer complexes between carbazole and lutetium bisphthalocyanine. New J Chem 2001;25:1148–51.
[39] Collman JP, Kendall JL, Chen JL, Collins KA, Marchon JC. Formation of charge-transfer complexes from neutral bis(porphyrin) sandwiches. Inorg Chem 2000;39:1661–7.
[40] Girolami GS, Hein CL, Suslick KS. A zirconium bis (porphyrinate) sandwich complex with an appended quinone. Angew Chem Int Ed 1996;35:1223–5.
[41] Buchler JW, Heinz G. Metal complexes with tetrapyrrole ligands, LXXII cerium(IV) sandwich complexes with porphyrin ligands linked by aliphatic and quinone-containing bridges. Chem Ber 1996;129:1073–81.
[42] Bian Y, Chen X, Wang D, Choi C-F, Zhou Y, Zhu P, et al. Porphyrin-appended europium(III) bis(phthalocyaninato) complexes. Synthesis, characterization, and photophysical properties. Chem Eur J 2007;13:4169–77.
[43] Ballesteros B, Torre G, Sharer A, Hausmann A, Herranz MÁ, Guldi DM, et al. Lanthanide(III) bisphthalocyaninato-[60]fullerene dyads: synthesis, characterization and photophysical properties. Chem Eur J 2010;16:114–25.
[44] Zhang X, Li Y, Qi D, Jiang J, Yan X, Bian Y. Linkage dependence of intramolecular fluorescence quenching process in porphyrin-appended mixed (phthalocyaninato)(porphyrinato) yttrium(III) double-decker complexes. J Phys Chem B 2010;114:13143–51.
[45] Stites JG, McCarty CN, Quill LL. The rare earth metals and their compounds. VIII. An improved method for the synthesis of some rare earth acetylacetonates. J Am Chem Soc 1948;70:3142–3.
[46] Rager C, Schmid G, Hanack M. Influence of substituents, reaction conditions and central metals on the isomer distributions of 1(4)-tetrasubstituted phthalocyanines. Chem Eur J 1999;5:280–8.
[47] Little RG. The synthesis of covalently linked tetraarylporphyrin dimers. J Heterocyclic Chem 1978;15:203–8.
[48] Feng J, Liang B, Wang D, Wu H, Xue L, Li X. Synthesis and aggregation behavior of perylenetetracarboxylic diimide trimers with different substituents at bay positions. Langmuir 2008;24:11209–15.
[49] Wang R, Li R, Li Y, Zhang X, Zhu P, Lo PC, et al. Controlling the nature of mixed (phthalocyaninato)(porphyrinato) rare-earth(III) double-decker complexes: the effects of nonperipheral alkoxy substitution of the phthalocyanine ligand. Chem Eur J 2006;12:1475–85.
[50] Zhang X, Muranaka A, Lv W, Zhang Y, Bian Y, Jiang J, et al. Optically active mixed phthalocyaninato–porphyrinato rare-earth double-decker complexes: synthesis, spectroscopy, and solvent-dependent molecular conformations. Chem Eur J 2008;14:4667–74.
[51] Zhou Y, Zhang Y, Wang H, Jiang J, Bian Y, Muranaka A, et al. Mixed (phthalocyaninato)(porphyrinato) rare earth double-decker complexes with C_4 chirality: synthesis, resolution, and absolute configuration assignment. Inorg Chem 2009;48:8925–33.
[52] Guyon F, Pondaven A, Guenot P, L'Her M. Bis(2,3-naphthalocyaninato)lutetium(III) and (2,3-naphthalocyaninato)- (phthalocyaninato)lutetium(III) complexes: synthesis, spectroscopic characterization, and electrochemistry. Inorg Chem 1994;33:4787–93.
[53] Zhang X, Bian Y, Jiang J. Synthesis, electrochemical and spectroscopic properties of C_{60}-porphyrin dyads with different phenyl ether linkage. Chin J Inorg Chem 2010;26:1719–28.